




OPEN The potential crosstalk genes and molecular mechanisms between glioblastoma and periodontitis

Jian-huang Huang^{1,2}, Yao Chen^{1,2}, Yuan-bao Kang¹, Zheng-jian Yao¹ & Jian-hua Song¹

Despite clinical and epidemiological evidence suggestive of a link between glioblastoma (GBM) and periodontitis (PD), the shared mechanisms of gene regulation remain elusive. In this study, we identify differentially expressed genes (DEGs) that overlap between the GEO datasets GSE4290 [GBM] and GSE10334 [PD]. Functional enrichment analysis was conducted, and key modules were identified using protein–protein interaction (PPI) network and weighted gene co-expression network analysis (WGCNA). The expression levels of CXCR4, LY96, and C3 were found to be significantly elevated in both the test dataset and external validation dataset, making them key crosstalk genes. Additionally, immune cell landscape analysis revealed elevated expression levels of multiple immune cells in GBM and PD compared to controls, with the key crosstalk genes negatively associated with Macrophages M2. FLI1 was identified as a potential key transcription factor (TF) regulating the three key crosstalk genes, with increased expression in the full dataset. These findings contribute to our understanding of the immune and inflammatory aspects of the comorbidity mechanism between GBM and PD.

Keywords Glioblastoma, Periodontitis, Crosstalk genes, Immune infiltration, Bioinformatics analysis

Glioblastoma (GBM) is a highly aggressive primary brain tumor and one of the deadliest and most recurrent solid tumors¹, accounting for 57% of all gliomas and 48% of primary central nervous system malignancies². Despite comprehensive treatment regimens including surgery, chemotherapy, and radiotherapy, the median survival of GBM patients after diagnosis is only about 15 months, with a 5-year survival rate of less than 10%³. Therefore, investigating the pathogenesis of GBM, particularly the study of modifiable risk factors for GBM progression, is crucial to improve the prognosis of GBM patients.

Periodontitis (PD), primarily caused by *Porphyromonas gingivalis*, is a chronic inflammatory disease marked by the gradual destruction of periodontal tissue⁴. During the active phase of PD, *Porphyromonas gingivalis* partially breaches the periodontal tissue, enters the bloodstream, and causes bacteremia. This leads to the release of numerous inflammatory mediators, ultimately provoking a prolonged low-grade inflammatory response in distant organs⁵. Chronic inflammation is widely believed to be associated with tumor formation and progression. Studies indicate that periodontitis elevates the risk of oral⁶, liver⁷, and colorectal cancers⁸ and is correlated with an increased overall cancer mortality rate⁹. In recent years, research has increasingly focused on the interaction between glioblastoma (GBM) and periodontitis (PD). Investigative studies have found that glioma patients exhibit significantly poorer periodontal health and a higher incidence of periodontitis compared to the general population¹⁰. Experimental studies further show that *Porphyromonas gingivalis* or its lipopolysaccharide (LPS) can cross the blood–brain barrier, enter brain tissue, and stimulate the proliferation and migration of glioma cells at varying concentrations¹¹. *Porphyromonas gingivalis* is not only linked to glioma grading but also shows a significant correlation with IDH1 (isocitrate dehydrogenase 1) mutations in gliomas¹². These mutations are crucial prognostic factors in glioma patients. These findings indicate that periodontal pathogens may have a significant role in glioma development. Nevertheless, the precise mechanisms through which periodontitis contributes to the initiation and progression of glioblastoma remain incompletely understood.

In this study, we utilized public datasets from the GEO database and TCGA-GBM to conduct bioinformatics analyses including differential expression gene (DEG) identification, functional enrichment analysis, weighted gene co-expression network analysis (WGCNA), and the Cibersort algorithm. The aim of this study

¹Department of Neurosurgery, Affiliated Hospital of Putian University, Putian, Fujian, China. ²These authors contributed equally: Jian-huang Huang and Yao Chen. ✉email: teamhuang@ptu.edu.cn

is to explore the common pathogenesis of glioblastoma (GBM) and periodontitis (PD), to provide new insights and approaches for controlling the development and progression of gliomas, as well as for the treatment of glioblastoma.

Materials and methods

Data sources

The study's flowchart is depicted in Fig. 1. The expression data for GBM and PD were obtained from the Gene Expression Omnibus (GEO) database (<https://www.ncbi.nlm.nih.gov/geo>). The search strategy for the GEO dataset included the following: (1) topic search for “glioblastoma” and “periodontitis,” respectively; (2) study type selection as “Expression profiling by array”; (3) samples were derived from Homo sapiens; and (4) the dataset contained normal control group samples. Based on the study design, the GEO datasets GSE4290 [GBM] and GSE10334 [PD] were used as the test set, with the former retaining only 23 normal samples and 81 GBM samples, and the latter containing 183 PD-affected gingival tissue samples and 64 unaffected gingival tissue samples.

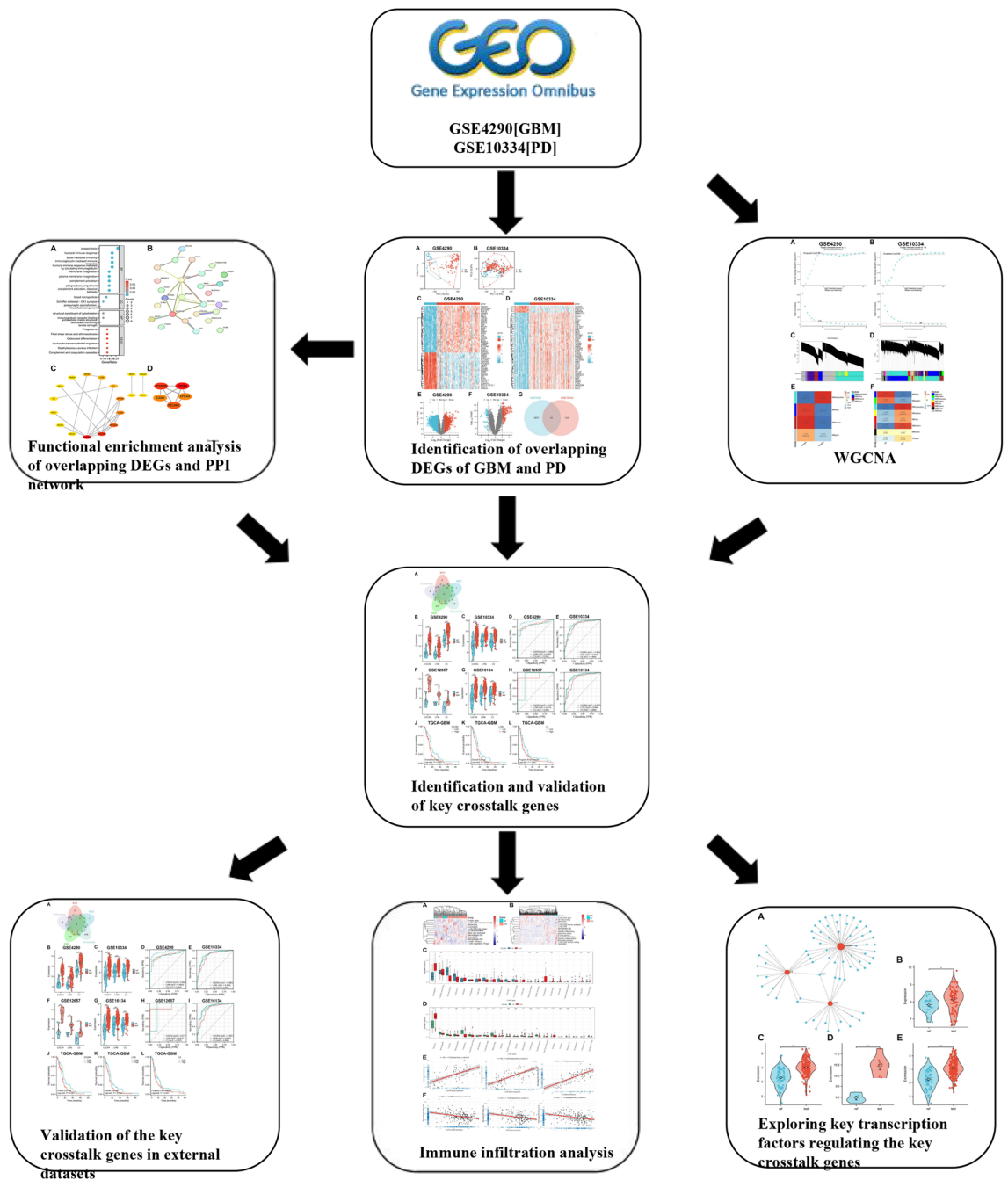


Figure 1. The flow diagram for the whole study.

Differentially expression analysis

The preliminary analyses of the dataset in this study were conducted using R software (version 4.2.0). The required disease and control samples were extracted according to the research needs. If the expression data had not been log₂ transformed, it was manually log₂ transformed. To identify the differentially expressed genes (DEGs) using the ‘Limma’ package¹³, the expression levels were normalized using the ‘normalizeBetweenArrays’ function to eliminate batch differences. Genes with a |log₂ fold change| > 1 and an adjusted P-value < 0.05 were identified as DEGs. Overlapping DEGs, which were up-regulated or down-regulated in both sets of DEGs, were defined. Venn plots of overlapping DEGs were created using the “ggvenn” package.

Enrichment analysis of overlapping DEGs

To analyze the overlapping DEGs, we employed the “clusterProfiler” package to conduct Gene Ontology (GO) and Kyoto Encyclopedia of Genes and Genomes (KEGG) enrichment analyses^{14,15}. Only terms with an FDR < 0.05 were considered to be significantly enriched.

Protein–protein interaction (PPI) network construction

To construct a PPI network with overlapping DEGs, we utilized the STRING database V11.5 (available at <http://string-db.org>). We set the “minimum required interaction score” parameter to 0.4 to exclude unconnected nodes. The resulting PPI network was then imported into Cytoscape software V3.9.1¹⁶ for visualization. To filter clusters with high connectivity, we employed the MCODE plug-in and used default parameters to divide the PPI network into multiple clusters. The CytoHubba plugin utilizes eleven node ranking methods to assess the significance of nodes within a biological network. These methods comprise Degree, Edge Percolated Component, Maximum Neighborhood Component, Density of Maximum Neighborhood Component, Maximal Clique Centrality, Bottleneck, EcCentricity, Closeness, Radiality, Betweenness, and Stress¹⁷. To provide a comprehensive evaluation of these genes, we employed both local methods (MCC) and global methods (EPC and EcCentricity). Local methods solely focus on the relationship between a node and its immediate neighbors, whereas global methods assess the node’s relationship with the entire network. Finally, we analyzed the genes within the clusters for functional enrichment.

Weighted gene co-expression network analysis (WGCNA)

The top 5000 genes with the highest absolute median difference in expression in the test dataset were screened for WGCNA analysis using the “WGCNA” package¹⁸. To begin, a soft threshold was obtained using the pickSoft-Threshold function. Next, a weighted adjacency matrix was constructed. Finally, the correlation between each module and the disease was calculated. The module with the highest correlation with the grouped traits was identified as the key module.

Identification and validation of key crosstalk genes

Firstly, we utilized Cytoscape software’s CytoHubba plugin¹⁷ to identify the hub genes in the PPI network. The genes that were ranked in the top 10 using various algorithms were determined as the PPI key genes. Subsequently, the PPI key genes were intersected with the key module genes of WGCNA, and these intersected genes were designated as the key crosstalk genes. We then compared the mRNA expression levels of the key crosstalk genes between the case and control groups using the Mann–Whitney *U* test. The results were considered statistically significant if the P value was less than 0.05, which was visualized using the “ggplot2” package. Finally, we evaluated the diagnostic efficacy of the key crosstalk genes in the test dataset by constructing receiver operating characteristic (ROC) curves using the “pROC” package.

Validation of key crosstalk genes in an independent external dataset

To validate the mRNA expression levels of key crosstalk genes, we utilized independent external datasets GSE14805 [GBM] and GSE16134 [PD]. In this study, GSE14805 included 4 control samples and 34 GBM samples. GSE16134 contained 241 PD-affected gingival tissue samples and 69 unaffected gingival tissue samples.

Immune infiltration analysis

First, immune cell expression levels in the test dataset were analyzed in the case and control groups using the “cibersort” algorithm¹⁹. Then, we calculated the correlation between key crosstalk gene expression and immune cell expression. We used the Spearman method to calculate the correlation coefficient and P-value between genes and immune cells. *P* < 0.05 was considered statistically significant and was visualized by “ggplot2”.

Identification of transcription factors (TFs) of key crosstalk genes

The TFs of key crosstalk genes were predicted by NetworkAnalyst 3.0 (available at <https://www.networkanalyst.ca>). We compared the average expression levels of these TFs in samples between different groups using the Mann–Whitney *U* test in both the test set and validation set. The results showed that TFs that were usually upregulated in the case group were identified as potential key TFs in GBM and PD.

Results

Identify overlapping DEGs of GBM and PDs

This study obtained satisfactory expression data through data preprocessing and normalization (Supplementary Fig. 1). PCA was used to downscale the mRNA expression data of the two test datasets, revealing significant differences between the case and control groups with good sample homogeneity (Fig. 2A–D). The “Limma”

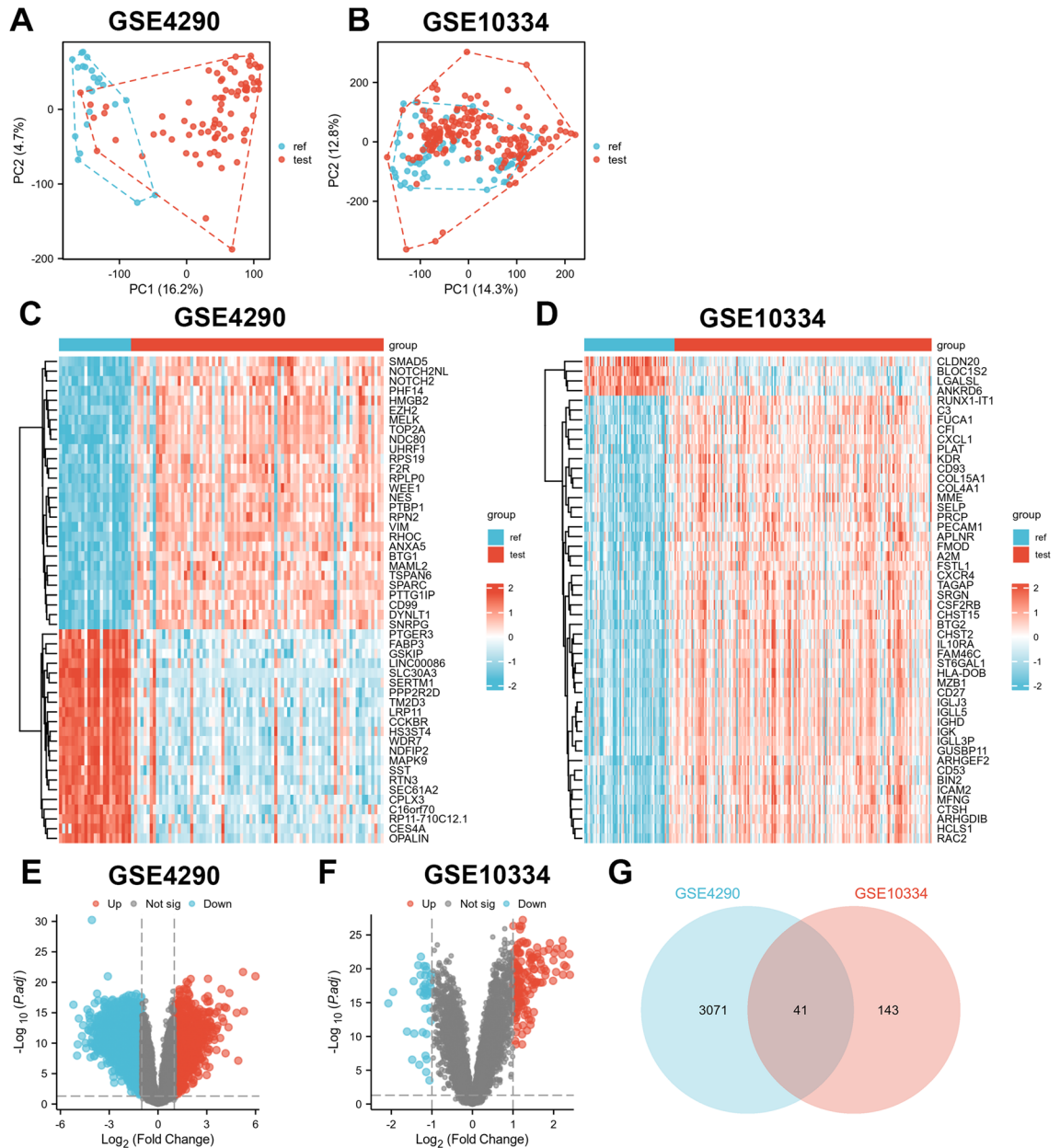


Figure 2. DEGs of test datasets GSE4290 and GSE10334. (A), (C), and (E) are PCA plots, heat maps, and volcano plots of GSE4290 differential gene analysis, respectively. (B), (D), and (F) are PCA plots, heat maps, and volcano plots of GSE10334 DEG analysis, respectively. (G) DEGs of GSE4290 and GSE10334 were crossed to obtain 41 crossover DEGs.

R package identified 3112 DEGs in dataset GSE4290, of which 1193 were up-regulated and 1919 were down-regulated (Fig. 2E). In dataset GSE10334, the “Limma” R package identified 184 DEGs, of which 146 were up-regulated and 38 were down-regulated (Fig. 2F). Subsequently, intersecting DEGs were identified (Fig. 2G), and the expression trends of these genes were examined, resulting in the identification of 30 overlapping DEGs.

Functional enrichment analysis of overlapping DEGs

We performed a functional enrichment analysis of the overlapping DEGs (Fig. 3A). Gene Ontology Biological Process (GO_BP) analysis revealed that the most significantly enriched terms were phagocytosis, humoral immune response-mediated circulating immunoglobulins, complement activation (classical pathway), immunoglobulin-mediated immune response, B cell-mediated immunity, and phagocytosis. KEGG analysis revealed that overlapping DEGs may be associated with complement and coagulation cascades, *Staphylococcus aureus* infection, leukocyte transendothelial migration, osteoclast differentiation, fluid shear stress, atherosclerosis, and phagosome. Therefore, it is clear that the functions of overlapping DEGs are strongly associated with immune and inflammatory processes.

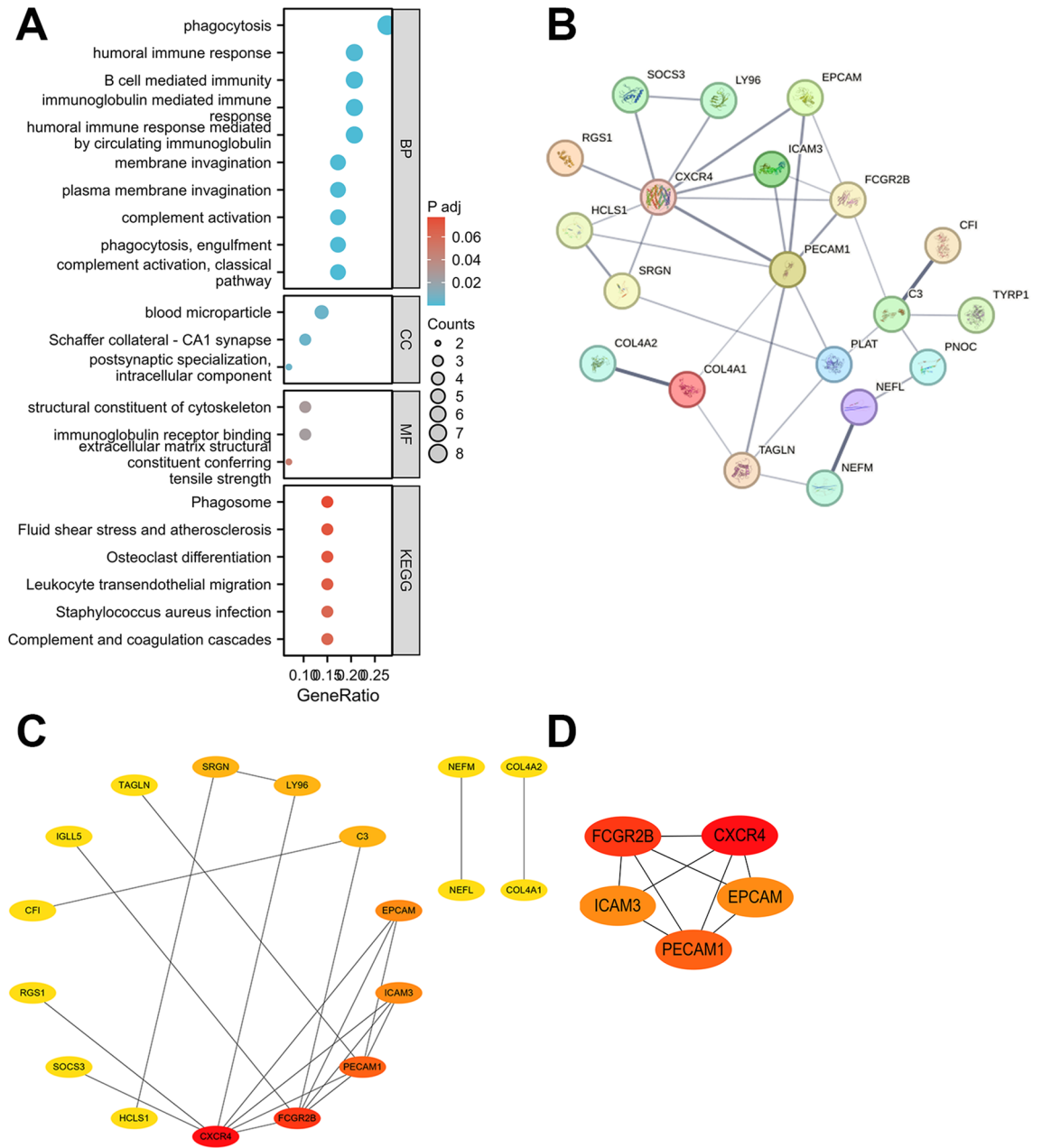


Figure 3. Functional enrichment analysis of overlapping DEGs and PPI network construction for the test dataset. **(A)** Functional enrichment analysis of overlapping DEGs. **(B)** PPI network constructed by overlapping DEGs. The thickness of the line represents the interaction intensity, and the thicker it is, the greater the interaction intensity. **(C)** Network construction of overlapping DEGs by Degree algorithm. The redder the color, the larger the Degree value. **(D)** PPI network obtained by Mcode algorithm for cluster 1.

Building PPI networks with overlapping DEGs

A PPI network with 28 nodes and 32 edges (PPI enrichment P-value < 1.5e-11) was constructed by entering the overlapping DEGs into the STRING database (Fig. 3B). The PPI network was visualized using Cytoscape software (Fig. 3C). A cluster with high connectivity was identified by the Mcode plug-in (Fig. 3D). This cluster contained 5 nodes, 9 edges and a score of 4.500. The genes included are CXCR4, EPCAM, FCGR2B, PECAM1, and ICAM3.

WGCNA construction and key module screening

WGCNA analysis was performed using the top 5000 genes with the highest absolute median difference in expression in the test dataset. $\beta = 8$ and $\beta = 18$ (scale-free $R^2 = 0.85$) were chosen as soft thresholds for GBM and PD, respectively, to ensure scale-free networks (Fig. 4A,B). WGCNA analysis identified 4 modules in GSE4290 and 8 modules in GSE10334 (Fig. 4C,D). Finally, a heat map of module-trait relationships was generated based on Pearson correlation coefficients. The results showed that the brown module had the highest correlation with

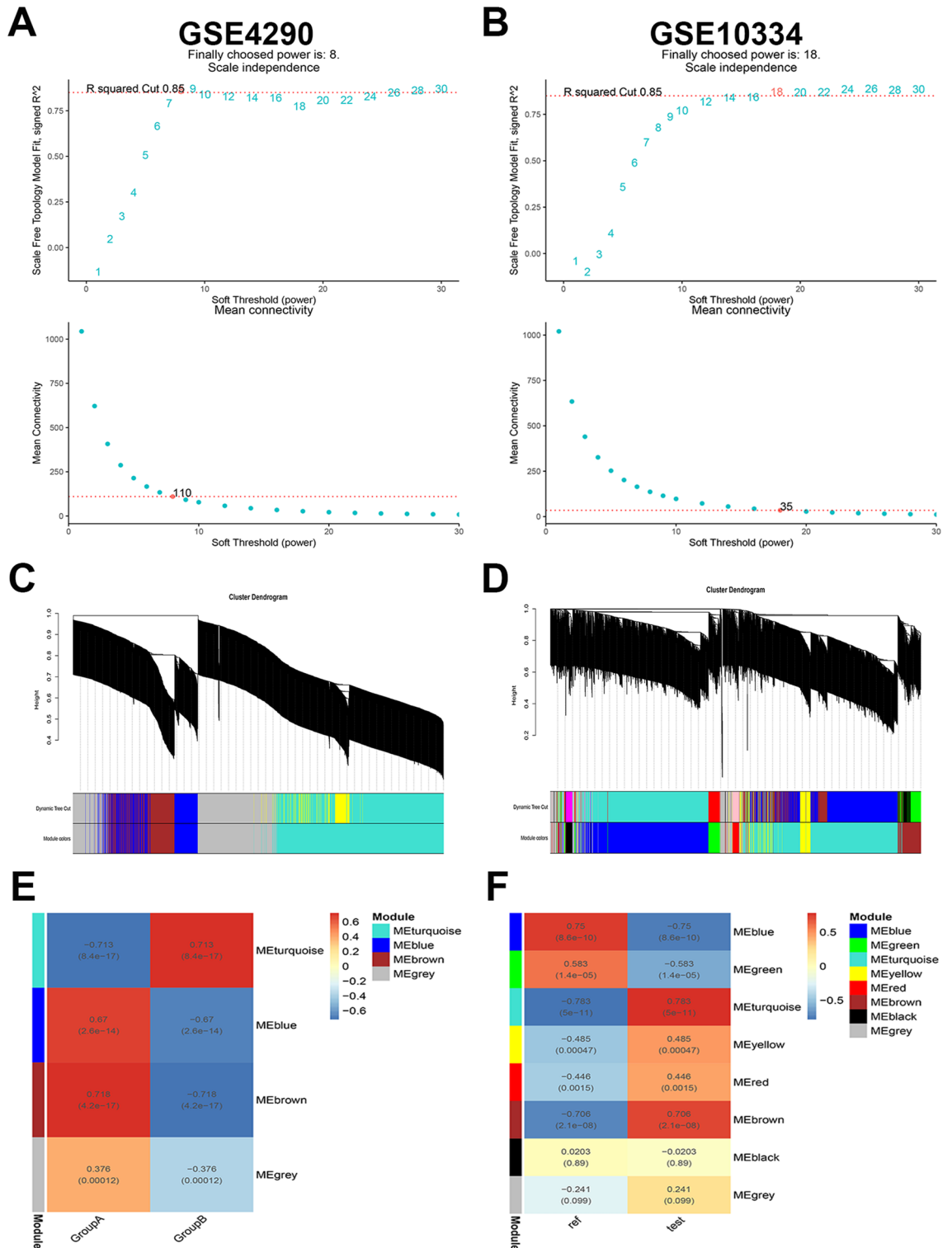


Figure 4. Weighted gene co-expression network analysis (WGCNA) of the test dataset. (A,B) Soft threshold selection for GSE4290 and GSE10334. (C,D) Clustering dendrogram of the top 5000 genes with the highest absolute median difference in expression between GSE4290 and GSE10334 based on differential measures. (E,F) Module-trait relationship between GSE4290 and modules of GSE10334 in relation to traits. Different colors represent different modules and contain the corresponding correlations and P-values.

GBM (0.718, $P = 4.2E-17$) and contained 272 genes; the turquoise module had the highest correlation with PD (0.783, $P = 5E-11$) and included 705 genes (Fig. 4E,F).

Identification and validation of key crossstalk genes

We employed the CytoHubba plugin to sort the top 10 genes under the Maximal Clique Centrality (MCC), Edge Percolated Component (EPC) and Eccentricity (EC) algorithms²². The Venn diagram revealed that CXCR4, LY96, and C3 were present in both the top 10 genes of the three algorithms and in the two key modules (Fig. 5A). Consequently, these three genes were identified as key crossstalk genes. In GSE4290 and GSE10334, mRNA expression levels of CXCR4, LY96, and C3 were significantly higher in the case group than in the control group (Fig. 5B,C). Moreover, CXCR4, LY96, and C3 exhibited satisfactory diagnostic ability for GBM and PD based on ROC curves, with AUC values exceeding 0.8 (Fig. 5D,E).

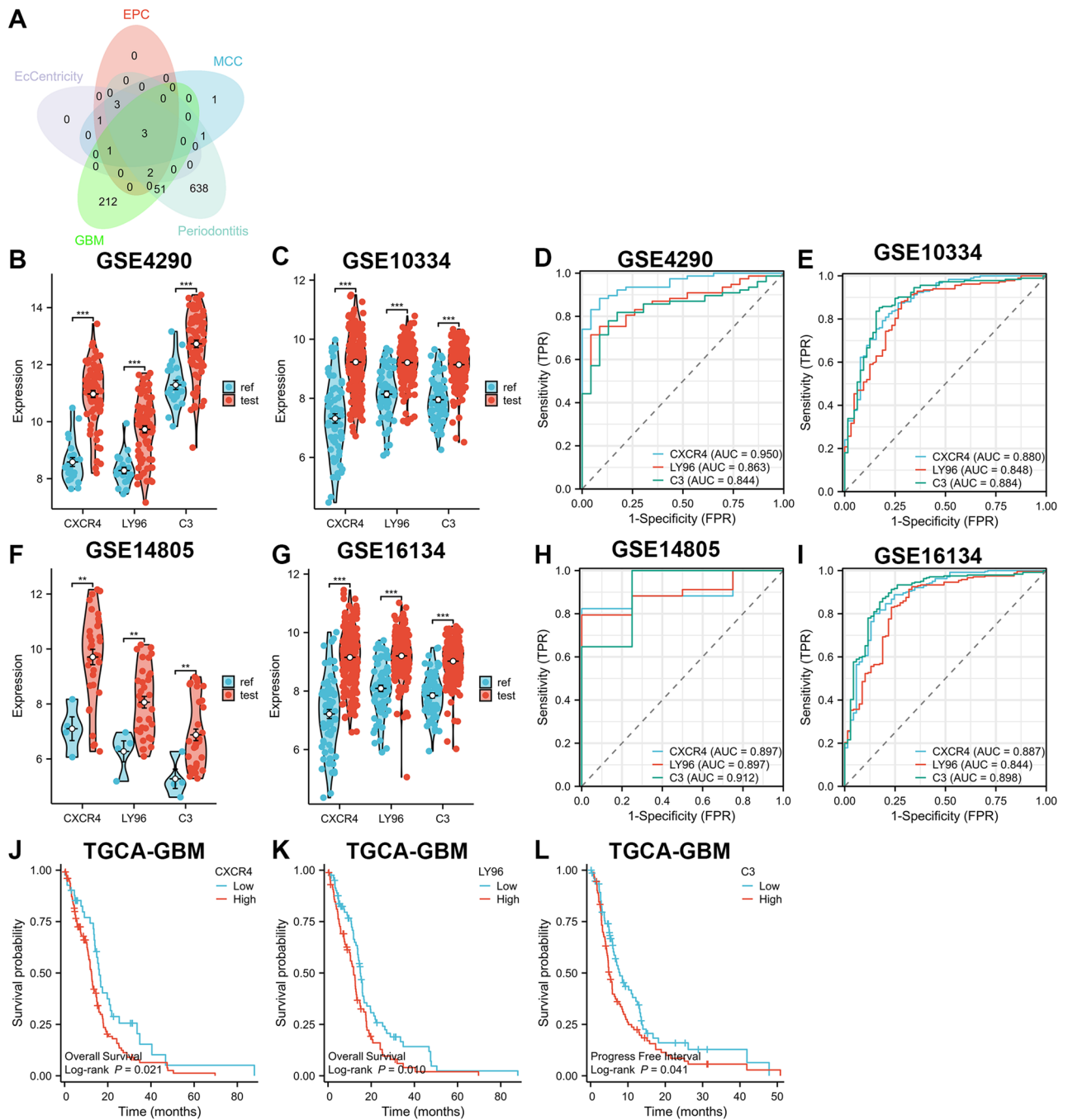


Figure 5. Identification and validation of key crossstalk genes. (A) CXCR4, LY96 and C3 mRNA are present in all three algorithms and two WGCNA key modules. (B,C) In the test set, CXCR4, LY96 and C3 mRNA expression levels are significantly higher in the case group than in the control group. (D,E) In the test set, CXCR4, LY96 and C3 have good diagnostic ability for GBM and PD. (F,G) In the validation set, CXCR4, LY96 and C3 mRNA expression levels were significantly higher in the case group than in the control group. (H,I) In the validation set, CXCR4, LY96 and C3 were diagnostically good for GBM and PD. (J–L) The TGCA-GBM dataset explores the prognosis of CXCR4, LY96 and C3 and GBM relationship. ***P < 0.0001. *P < 0.01.

Validation of key crosstalk genes in an independent external dataset

To increase the confidence level, we validated the expression of key crosstalk genes in two other independent external datasets (GSE14805 [GBM] and GSE16134 [PD]). The expression differences were consistent with the test set (Fig. 5F,G), while demonstrating good diagnostic efficiency (Fig. 5H,I). Subsequently, we analyzed using the TCGA-GBM dataset and discovered that high expression of CXCR4, LY96, and C3 was associated with poor prognosis of GBM (Fig. 5J–L).

Immuno-infiltration analysis

By conducting an enrichment analysis of overlapping DEGs, we found that immune and inflammatory processes are involved in the crosstalk between GBM and PD. Therefore, we utilized the ciphersort algorithm to analyze the proportion of immune cells in the case group versus control samples in both test datasets. We found a significantly altered immune landscape in GBM and PD in the case group, with a reciprocal trend in Macrophages M2 (Fig. 6A–D). Correlation analysis demonstrated that CXCR4, LY96, and C3 expression levels were significantly and positively correlated with Macrophages M2 in GBM (Fig. 6E), and the opposite in PD (Fig. 6F). Subsequently, we further validated the above results using an external validation set (supplementary materials—Fig. 2).

Exploring key transcription factors (TFs) that regulate key crosstalk genes

Furthermore, we examined potential transcription factors that may regulate CXCR4, LY96, and C3 genes using NetworkAnalyst 3.0 and compared the expression levels of case and control groups in all datasets using the Mann–Whitney *U* test. We discovered that FLI-1 interacted with CXCR4, LY96, and C3 simultaneously (Fig. 7A) and that FLI-1 expression levels were significantly elevated in all case groups (Fig. 7B–E). Therefore, FLI-1 may be a potential key transcription factor regulating two crucial crosstalk genes in the pathological process of GBM and PD.

Discussion

Both GBM and PD are prevalent health issues that often impose a significant burden on families and society. Previous reports have suggested a strong association between GBM and PD¹¹. However, the specific pathogenic mechanism and crosstalk genes remain unclear. In this study, we conducted a bioinformatics analysis of the crosstalk between GBM and PD. Our findings revealed that CXCR4, LY96, and C3 genes play a crucial role in the co-pathogenesis of both diseases. Furthermore, we explored the transcription factors of crosstalk genes and discovered that Friend leukemia integration 1 (FLI1) regulates the above three crosstalk genes simultaneously. This study provides a new direction for future research on the relationship between periodontitis and the onset and progression of GBM as well as targeted therapy. It is worth noting that this study may be the first literature to report crosstalk genes between GBM and PD.

Chemokine (C-X-C motif) receptor 4 (CXCR4), a G protein-coupled receptor, binds its typical ligand stromal cell-derived factor 1 (SDF-1). Although CXCR4 signaling is essential for individual development and organ repair²⁰, high CXCR4 expression has been linked to an increased risk of cancer²¹. The present study found that CXCR4 is overexpressed in GBM and is associated with a poorer prognosis²², consistent with previous findings. In GBM, ligand binding to CXCR4 induces conformational changes that activate PI3K-AKT, JAK/STAT, and MEK1/2-Erk1/2 pathways, leading to the activation of STAT3, an oncogenic transcription factor involved in GBM growth²³. Inhibition of MEK-ERK1/2 signaling enhances the adhesion of glioma cells to the ECM and reduces cell proliferation and migration²⁴. Additionally, CXCR4 was found to be overexpressed in periodontitis gingival tissue, as shown in this study²⁵. Activation of CXCR4 by *Porphyromonas gingivalis* leads to crosstalk with Toll-like receptor 2 (TLR2), which disrupts the killing function of monocytes or macrophages by inhibiting NO production and increasing cAMP-dependent protein kinase A (PKA) signaling²⁶. Furthermore, PI3K-dependent adhesion pathway activation via CXCR4 in monocytes and macrophages leads to CR3 activation, which is utilized by *Porphyromonas gingivalis* and other pathogens as a safe entry portal to enhance their intracellular survival²⁷.

Lymphocyte antigen 96 (LY96, MD2) is a crucial component required for the activation of TLR4 by LPS in the outer wall of *Porphyromonas gingivalis*. It serves as the first line of defense against microbial infection²⁸. LY96 expression is significantly elevated in gingival tissues of patients with periodontitis²⁹, resulting in the formation of TLR4-LY96-CD14 complexes that trigger the MyD88 pathway, leading to the production of tumor necrosis factor α , IL-6, IL-8, and IL-2³⁰. Recent studies have shown that LY96 is closely associated with tumorigenesis and progression in various cancers, including colon cancer³¹, and GBM³², with the highest expression being observed in GBM and predicting a worse prognosis^{33,34}. In GBM, TLR4 is usually expressed on glioma tissues and microglia/macrophages³⁵. The stimulation of TLR4/MD2 complex signaling by LPS may involve loss or mutation of the tumor suppressor PTEN³⁶, which can have a significant impact on cancer susceptibility and tumorigenesis, even with subtle changes in its function.

Complement C3 is a central component where classical, lectin, and alternative pathways converge, producing effector molecules such as C3a and C5a that activate C3aR and C5aR, respectively, leading to leukocyte mobilization and activation³⁷. Histological observations indicate that C3-activated complement fragments are abundant in the gingival crevices of periodontitis and positively correlate with inflammatory indices. After treatment of periodontitis, complement C3 levels significantly decrease (Top 5% genes), whereas they are absent or present at lower concentrations in healthy individuals³⁷. Mechanistically, C3 activation may promote periodontal inflammation mainly by increasing vascular permeability and chemotactic recruitment of inflammatory cells through activation of C5aR increasing vascular permeability and flow of inflammatory exudates and chemotactic recruitment of inflammatory cells³⁸, but it does not control infection³⁹. Therefore, C3 is currently identified as one of the 21 most promising candidate genes for periodontitis treatment⁴⁰. High levels of complement-activating proteins may be beneficial for tumors⁴¹. A study showed that C3 deposition was observed in GBM tissues, indicating

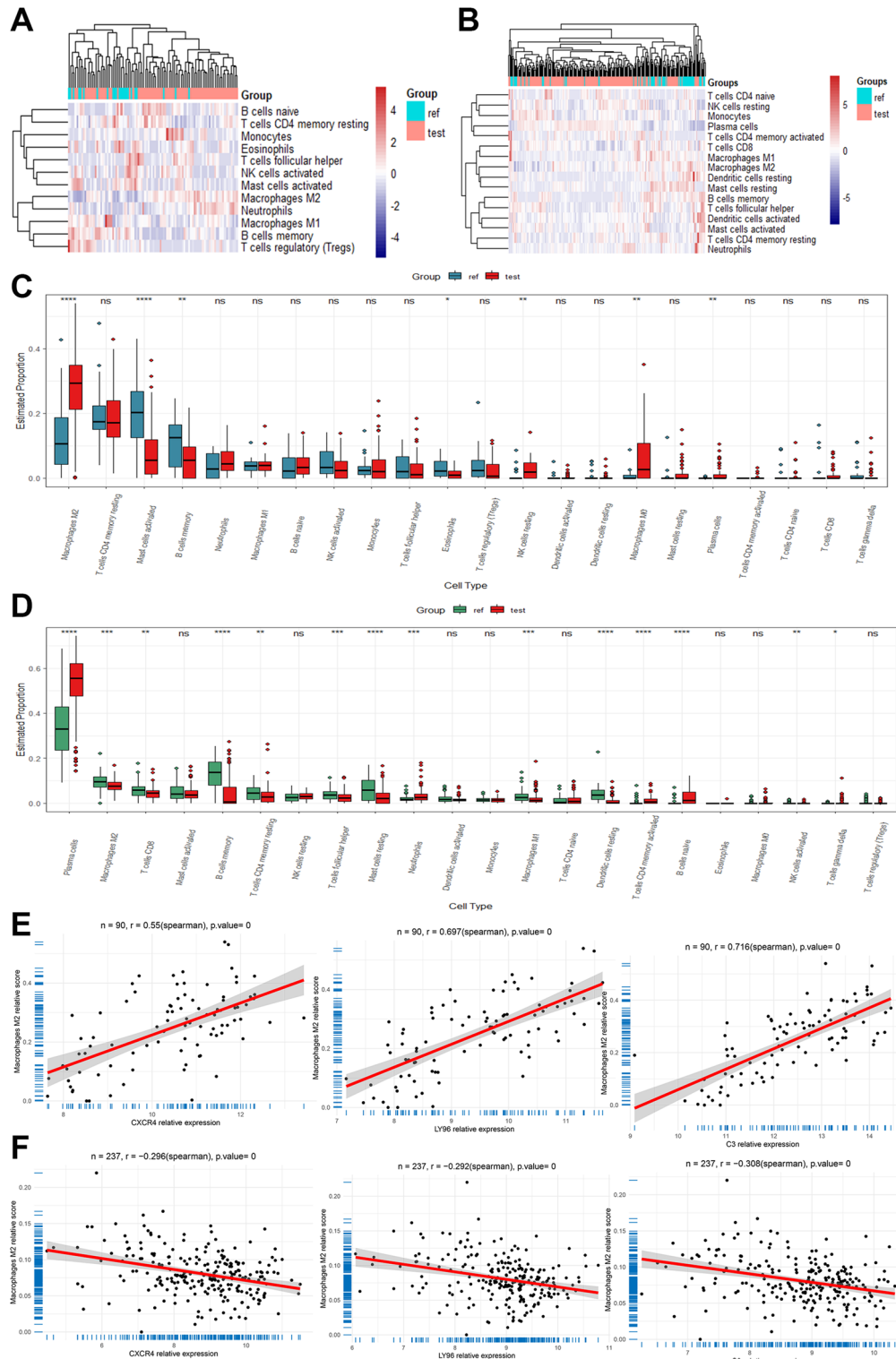


Figure 6. Immune infiltration analysis of the test dataset. (A,B) Immune landscape between groups in dataset GSE4290 and GSE10334. (C) Comparison of immune cell composition between case groups and controls in dataset GSE4290. (D) Comparison of immune cell composition between case groups and controls in dataset GSE10334. (E) CXCR4, LY96 and C3 expression levels in dataset GSE4290 are significantly positively correlated with Macrophages M2, LY96 and C3 expression levels were significantly and positively correlated with Macrophages M2 in dataset GSE4290. (F) CXCR4, LY96 and C3 expression levels were significantly and negatively correlated with Macrophages M2 in dataset GSE10334. ***P < 0.0001; **P < 0.001; *P < 0.01.

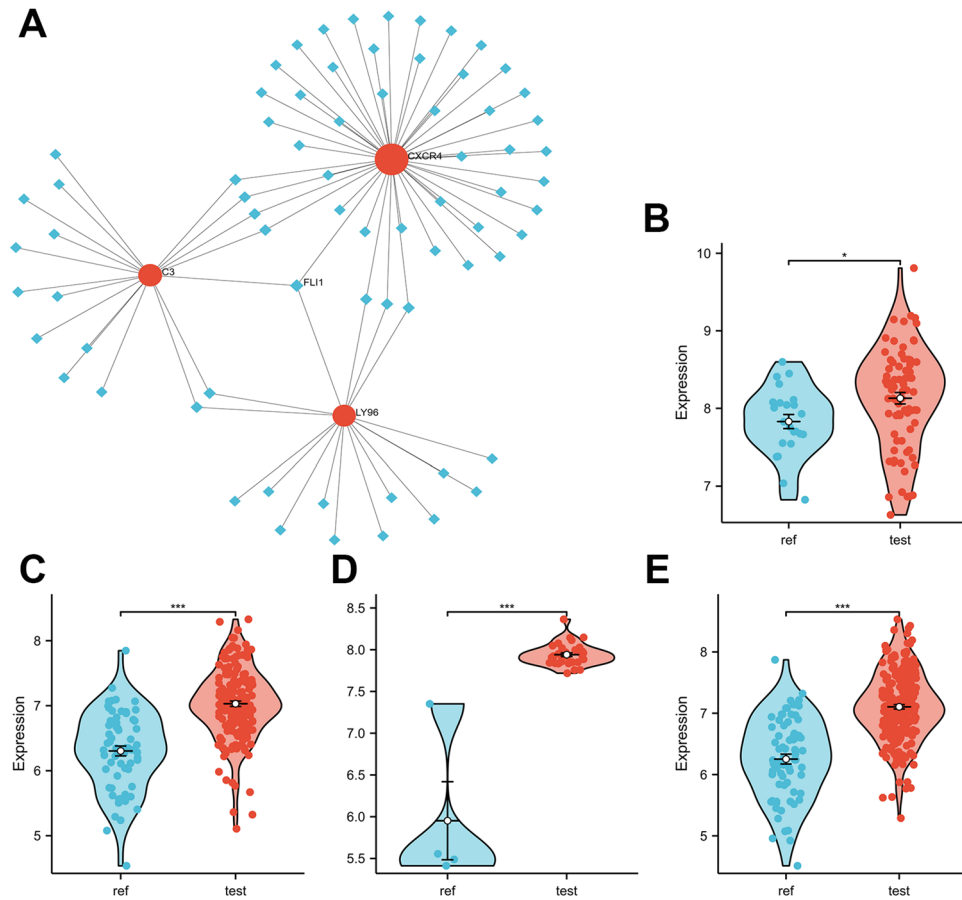


Figure 7. FLI1 is identified as a potential key TF shared in GBM and PD. (A) NetworkAnalyst 3.0 exploration suggests that FLI1 regulates both CXCR4, LY96 and C3 genes. (B,C) FLI1 was significantly elevated in the test dataset (GSE4290 and GSE10334) case set. (D,E) FLI1 was significantly elevated in the external validation dataset (GSE14805 and GSE16134) case set. * $P < 0.01$; ** $P < 0.001$; *** $P < 0.0001$.

local complement activation in GBM, and confirmed the protective effect of complement C3 on GBM development and progression⁴². It is important to note that glioma stem cells (GCS) may activate C3 with the help of alternative pathways and activate STAT-3, ERK2/1, and PI3K/Akt/mTOR pathways to maintain their pluripotent state⁴². Additionally, hypoxic conditions contribute to C3 activation and enhance C3a-C3aR effects⁴³, forming an additional effector mechanism for GSC survival, self-renewal, and tumor growth.

In our study, we identified characteristic genes shared by GBM and periodontitis that were closely associated with the immune process. Firstly, based on comprehensive bioinformatics analysis, we screened overlapping DEGs of GBM and PD mRNA expression profiles and found that these genes are mainly involved in complement and coagulation cascades, *Staphylococcus aureus* infection, leukocyte transendothelial migration, osteoclast differentiation, fluid shear stress, atherosclerosis, phagosome, and other immune-related biological pathways. Subsequently, we identified three crosstalk genes (CXCR4, LY96, and C3) in GBM and PD using a combined screen of PPI network, hub genes, and WGCNA analysis. It is worth emphasizing that all three genes are immune-related. The ROC analysis suggested that all three crosstalk genes showed high sensitivity and specificity, which was conclusively validated in the external validation dataset. Finally, we analyzed the immune characteristics of GBM and PD using immune infiltration. The study showed decreased macrophage M2 polarization in PD, which negatively correlated with key crosstalk gene expression and was consistent with a pro-inflammatory manifestation of PD⁴⁴. Increased macrophage M2 polarization in GBM positively correlated with key crosstalk gene expression and was consistent with an immunosuppressive tumor microenvironment in GBM⁴⁵. We speculate that the disparities in gene effects may primarily be attributed to the distinct cells in which interacting genes function and the secretion of various inflammatory factors. For instance, in GBM cells, the upregulation of CXCR4 recruits glioma-associated microglia/macrophages (GAMs) and results in M2 polarization of macrophages⁴⁶. Conversely, in periodontal inflammation, the upregulation of CXCR4 inhibits TLR4-induced NF- κ B activation through the LPS-CXCR4 axis, thereby suppressing M2 polarization of macrophages⁴⁷. Furthermore, it is also associated with the lack of other immune cell types, such as insufficiently activated CD8⁺ T cells and functionally impaired microglia in GBM^{48,49}.

These findings suggest that these shared DEGs may bridge the common pathogenesis of GBM and PD by affecting immune cells. We further explore the mechanism of crosstalk between PD and GBM. Firstly,

Porphyromonas gingivalis, the primary causative agent of PD, activates complement C3 or CXCR4, impairing the killing capacity of neutrophils and macrophages but failing to control infection^{37,39,50}. This is consistent with the results of functional enrichment analysis such as phagocytosis, complement activation (classical pathway), etc. As a result, *P. gingivalis* proliferates uncontrollably in an inflammatory environment. Secondly, *P. gingivalis* disseminates distantly with the bloodstream, this conforms to the results of functional enrichment analysis of Leukocyte transendothelial migration, Cell adhesion molecules, and others. Then, LPS binding to LY96 causes disruption of the blood–brain barrier, triggering chronic and insidious inflammation formation in the brain, promoting glial cell carcinogenesis and exacerbating tumor growth⁵¹. Specific mechanisms include loss/mutation of the tumor suppressor PTEN³⁶, maintenance and survival of GCS stemness⁴², and treatment resistance⁵². Although glioma-associated microglia and macrophages (GAMs) and MDSC are recruited into the glioma microenvironment and release various growth factors and cytokines, abnormal expression of CXCR4 and C3 leads to immunosuppression⁵³, resulting in restricted clearance of cancer cells.

To investigate the candidate regulatory mechanisms of GBM and PD crosstalk genes, we constructed a target gene-TF network. Our study revealed that Friend leukemia integration 1 transcription factor (FLI1) interacts closely with three crosstalk genes simultaneously. Currently, little is known about the role of FLI1 in GBM and PD. Only literature shows that FLI1 is overexpressed in GBM tissues and enhances GBM radiotherapy resistance⁵⁴. This finding is consistent with the results of our present study. However, further validation is needed in PD.

The current study identified key crosstalk genes and transcription factors (TFs) in GBM and PD from an immune and inflammatory perspective, thus providing new insight into the comorbidity mechanism of these diseases. It is important to note that the conclusions require further clinical validation in the future. Additionally, the specific functions of the crosstalk genes need to be validated in vivo and in vitro. Subsequently, we plan to establish reliable animal models to further validate these findings, which will require significant time and funding to advance our theory. Nevertheless, this work remains essential and worth pursuing.

Conclusion

In conclusion, we identified CXCR4, LY96, and C3 as key crosstalk genes in GBM and PD using multiple bioinformatics analysis methods. These genes may play a role in the crosstalk between these diseases through immune pathways. Furthermore, FLI1 was identified as a potential key transcription factor (TF) in IAs and PD. To our knowledge, this is the first study to report these findings. The current study provides new insights into the co-pathogenesis of GBM and PD, and further validation is required to confirm these results.

Data availability

The datasets analyzed in this study are available for download in the Gene Expression Omnibus (GEO) and TCGA-GBM dataset. GSE4290 dataset: <https://www.ncbi.nlm.nih.gov/geo/query/acc.cgi?acc=GSE4290>. GSE10334 dataset: <https://www.ncbi.nlm.nih.gov/geo/query/acc.cgi?acc=GSE10334>. GSE12657 dataset: <https://www.ncbi.nlm.nih.gov/geo/query/acc.cgi?acc=GSE12657>. GSE16134 dataset: <https://www.ncbi.nlm.nih.gov/geo/query/acc.cgi?acc=GSE16134>. TCGA-GBM dataset: [https://xenabrowser.net/datapages/?cohort=GDC%20TCGA%20Glioblastoma%20\(GBM\)&removeHub=https%3A%2F%2Fxcna.treehouse.gi.ucsc.edu%3A443](https://xenabrowser.net/datapages/?cohort=GDC%20TCGA%20Glioblastoma%20(GBM)&removeHub=https%3A%2F%2Fxcna.treehouse.gi.ucsc.edu%3A443).

Received: 14 July 2023; Accepted: 8 March 2024

Published online: 12 March 2024

References

- Alexander, B. M. & Cloughesy, T. F. Adult glioblastoma. *J. Clin. Oncol.* **35**, 2402–2409 (2017).
- Weller, M. & Le Rhun, E. How did lomustine become standard of care in recurrent glioblastoma?. *Cancer Treat. Rev.* **87**, 102029 (2020).
- Stupp, R. *et al.* Radiotherapy plus concomitant and adjuvant temozolomide for glioblastoma. *N. Engl. J. Med.* **352**, 987–996 (2005).
- Slots, J. Periodontitis: Facts, fallacies and the future. *Periodontology* **2000**(75), 7–23 (2017).
- Ding, F. *et al.* Detection of periodontal pathogens in the patients with aortic aneurysm. *Chin. Med. J. (Engl.)* **127**, 4114–4118 (2014).
- Kavarthapu, A. & Gurumoorthy, K. Linking chronic periodontitis and oral cancer: A review. *Oral Oncol.* **121**, 105375 (2021).
- Al-Maweri, S. A. *et al.* Association of periodontitis and tooth loss with liver cancer: A systematic review. *Crit. Rev. Oncol. Hematol.* **159**, 103221 (2021).
- Mesa, F. *et al.* A new comorbidity in periodontitis: *Fusobacterium nucleatum* and colorectal cancer. *Medicina (Kaunas)* **58**, 546 (2022).
- Heikkilä, P., But, A., Sorsa, T. & Haukka, J. Periodontitis and cancer mortality: Register-based cohort study of 68,273 adults in 10-year follow-up. *Int. J. Cancer* **142**, 2244–2253 (2018).
- Sun, H. *et al.* Prevalence and associated factors of periodontal conditions among 55- to 74-year-old adults in China: Results from the 4th National Oral Health Survey. *Clin. Oral Investig.* **24**, 4403–4412 (2020).
- Gao, Z. *et al.* *Porphyromonas gingivalis*-derived lipopolysaccharide promotes glioma cell proliferation and migration via activating Akt signaling pathways. *Cells* **11**, 4088 (2022).
- Wen, Y. *et al.* Association between oral microbiota and human brain glioma grade: A case–control study. *Front. Microbiol.* **12**, 746568 (2021).
- Ritchie, M. E. *et al.* limma powers differential expression analyses for RNA-sequencing and microarray studies. *Nucleic Acids Res.* **43**, e47 (2015).
- Ashburner, M. *et al.* Gene ontology: Tool for the unification of biology. The Gene Ontology Consortium. *Nat. Genet.* **25**, 25–29 (2000).
- Kanehisa, M. & Goto, S. KEGG: Kyoto encyclopedia of genes and genomes. *Nucleic Acids Res.* **28**, 27–30 (2000).
- Shannon, P. *et al.* Cytoscape: A software environment for integrated models of biomolecular interaction networks. *Genome Res.* **13**, 2498–2504 (2003).
- Chin, C. H. *et al.* cytoHubba: Identifying hub objects and sub-networks from complex interactome. *BMC Syst. Biol.* **8**(Suppl 4), S11 (2014).

18. Langfelder, P. & Horvath, S. WGCNA: An R package for weighted correlation network analysis. *BMC Bioinform.* **9**, 559 (2008).
19. Newman, A. M. *et al.* Robust enumeration of cell subsets from tissue expression profiles. *Nat. Methods* **12**, 453–457 (2015).
20. Das, S. *et al.* A unique collateral artery development program promotes neonatal heart regeneration. *Cell* **176**, 1128–1142.e11118 (2019).
21. Wu, Y. *et al.* CXC motif chemokine receptor 4 gene polymorphism and cancer risk. *Medicine (Baltimore)* **95**, e5317 (2016).
22. Khan, A. B. *et al.* CXCR4 expression is associated with proneural-to-mesenchymal transition in glioblastoma. *Int. J. Cancer* **152**, 713–724 (2023).
23. Le Rhun, E. *et al.* Molecular targeted therapy of glioblastoma. *Cancer Treat. Rev.* **80**, 101896 (2019).
24. Ramaswamy, P., Nanjiah, N. D. & Borkotokey, M. Role of MEK-ERK signaling mediated adhesion of glioma cells to extra-cellular matrix: Possible implication on migration and proliferation. *Ann. Neurosci.* **26**, 52–56 (2019).
25. Nagashima, H. *et al.* CXCR4 signaling in macrophages contributes to periodontal mechanical hypersensitivity in *Porphyromonas gingivalis*-induced periodontitis in mice. *Mol. Pain* **13**, 1744806916689269 (2017).
26. Pierce, D. L. *et al.* Host adhesive activities and virulence of novel fimbrial proteins of *Porphyromonas gingivalis*. *Infect. Immun.* **77**, 3294–3301 (2009).
27. Hajishengallis, G., McIntosh, M. L., Nishiyama, S. I. & Yoshimura, F. Mechanism and implications of CXCR4-mediated integrin activation by *Porphyromonas gingivalis*. *Mol. Oral Microbiol.* **28**, 239–249 (2013).
28. Dou, T. *et al.* Signatures of positive selection in LY96 gene in vertebrates. *J. Biosci.* **38**, 899–904 (2013).
29. Li, J. P. *et al.* Differential expression of Toll-like receptor 4 in healthy and diseased human gingiva. *J. Periodontol. Res.* **49**, 845–854 (2014).
30. Kawai, T. & Akira, S. Toll-like receptors and their crosstalk with other innate receptors in infection and immunity. *Immunity* **34**, 637–650 (2011).
31. Rajamanickam, V. *et al.* Selective targeting of the TLR4 co-receptor, MD2, prevents colon cancer growth and lung metastasis. *Int. J. Biol. Sci.* **16**, 1288–1302 (2020).
32. Zhao, M., Li, X., Chen, Y. & Wang, S. MD2 is a potential biomarker associated with immune cell infiltration in gliomas. *Front. Oncol.* **12**, 854598 (2022).
33. Nie, K., Li, J., Peng, L., Zhang, M. & Huang, W. Pan-cancer analysis of the characteristics of LY96 in prognosis and immunotherapy across human cancer. *Front. Mol. Biosci.* **9**, 837393 (2022).
34. Moretti, I. F. *et al.* Late p65 nuclear translocation in glioblastoma cells indicates non-canonical TLR4 signaling and activation of DNA repair genes. *Sci. Rep.* **11**, 1333 (2021).
35. Xun, Y., Yang, H., Kaminska, B. & You, H. Toll-like receptors and toll-like receptor-targeted immunotherapy against glioma. *J. Hematol. Oncol.* **14**, 176 (2021).
36. Moretti, I. F., Franco, D. G., de Almeida Galatro, T. F., Oba-Shinjo, S. M. & Marie, S. K. N. Plasmatic membrane toll-like receptor expressions in human astrocytomas. *PLoS One* **13**, e0199211 (2018).
37. Hajishengallis, G. Complement and periodontitis. *Biochem. Pharmacol.* **80**, 1992–2001 (2010).
38. Krauss, J. L., Potempa, J., Lambris, J. D. & Hajishengallis, G. Complementary Tolls in the periodontium: How periodontal bacteria modify complement and Toll-like receptor responses to prevail in the host. *Periodontology* **2000**(52), 141–162 (2010).
39. Delima, A. J. & Van Dyke, T. E. Origin and function of the cellular components in gingival crevice fluid. *Periodontology* **2000**(31), 55–76 (2003).
40. Zhan, Y. *et al.* Prioritization of candidate genes for periodontitis using multiple computational tools. *J. Periodontol.* **85**, 1059–1069 (2014).
41. Markiewski, M. M. & Lambris, J. D. Is complement good or bad for cancer patients? A new perspective on an old dilemma. *Trends Immunol.* **30**, 286–292 (2009).
42. Bouwens, T. A. *et al.* Complement activation in glioblastoma multiforme pathophysiology: Evidence from serum levels and presence of complement activation products in tumor tissue. *J. Neuroimmunol.* **278**, 271–276 (2015).
43. Pedersen, E. D. *et al.* Expression of complement regulators and receptors on human NT2-N neurons—Effect of hypoxia and reoxygenation. *Mol. Immunol.* **44**, 2459–2468 (2007).
44. Almubarak, A., Tanagala, K. K. K., Papapanou, P. N., Lalla, E. & Momen-Heravi, F. Disruption of monocyte and macrophage homeostasis in periodontitis. *Front. Immunol.* **11**, 330 (2020).
45. Walters, M. J. *et al.* Inhibition of CXCR7 extends survival following irradiation of brain tumours in mice and rats. *Br. J. Cancer* **110**, 1179–1188 (2014).
46. Mercurio, L. *et al.* Targeting CXCR4 by a selective peptide antagonist modulates tumor microenvironment and microglia reactivity in a human glioblastoma model. *J. Exp. Clin. Cancer Res.* **35**, 55 (2016).
47. Lin, Y. H. *et al.* Interleukin 26 skews macrophage polarization towards M1 phenotype by activating cJUN and the NF- κ B pathway. *Cells* **9**, 938 (2020).
48. Qian, J. *et al.* TLR2 promotes glioma immune evasion by downregulating MHC class II molecules in microglia. *Cancer Immunol. Res.* **6**, 1220–1233 (2018).
49. Locarno, C. V. *et al.* Role of myeloid cells in the immunosuppressive microenvironment in gliomas. *Immunobiology* **225**, 151853 (2020).
50. Hajishengallis, G. & Lambris, J. D. Microbial manipulation of receptor crosstalk in innate immunity. *Nat. Rev. Immunol.* **11**, 187–200 (2011).
51. Balkwill, F. & Mantovani, A. Inflammation and cancer: Back to Virchow?. *Lancet* **357**, 539–545 (2001).
52. Liu, S. C. *et al.* Blockade of SDF-1 after irradiation inhibits tumor recurrences of autochthonous brain tumors in rats. *Neuro Oncol.* **16**, 21–28 (2014).
53. Hambarzumyan, D., Gutmann, D. H. & Kettenmann, H. The role of microglia and macrophages in glioma maintenance and progression. *Nat. Neurosci.* **19**, 20–27 (2016).
54. Rajesh, Y. *et al.* Transcriptional regulation of HSPB1 by Friend leukemia integration-1 factor modulates radiation and temozolomide resistance in glioblastoma. *Oncotarget* **11**, 1097–1108 (2020).

Author contributions

J.H analyzed the data and wrote this manuscript. Y.C, Y.K and J.S assisted in analyzing the data and revising the manuscript. Y.C, Z.Y critically read and edited the manuscript. All authors reviewed the manuscript.

Competing interests

The authors declare no competing interests.

Additional information

Supplementary Information The online version contains supplementary material available at <https://doi.org/10.1038/s41598-024-56577-2>.

Correspondence and requests for materials should be addressed to J.H.

Reprints and permissions information is available at www.nature.com/reprints.

Publisher's note Springer Nature remains neutral with regard to jurisdictional claims in published maps and institutional affiliations.



Open Access This article is licensed under a Creative Commons Attribution 4.0 International License, which permits use, sharing, adaptation, distribution and reproduction in any medium or format, as long as you give appropriate credit to the original author(s) and the source, provide a link to the Creative Commons licence, and indicate if changes were made. The images or other third party material in this article are included in the article's Creative Commons licence, unless indicated otherwise in a credit line to the material. If material is not included in the article's Creative Commons licence and your intended use is not permitted by statutory regulation or exceeds the permitted use, you will need to obtain permission directly from the copyright holder. To view a copy of this licence, visit <http://creativecommons.org/licenses/by/4.0/>.

© The Author(s) 2024